

# Granular superconductivity in the cuprates evinced by finite size effects in the specific heat and London penetration depths

T. Schneider

*Physik-Institut der Universität Zürich, Winterthurerstrasse 190,  
CH-8057 Zürich, Switzerland*

We review and refine the finite size scaling analysis of specific heat and London penetration depths data of cuprate superconductors and compare it to the analysis of specific heat measurements near the superfluid transition of  $^4\text{He}$  confined to  $1\mu\text{m}^3$  cylindrical boxes. This system crosses from  $3D$  to  $0D$  behavior near the transition. This has a marked effect on the specific heat as seen by a pronounced rounding of the maximum and a shift to a temperature lower than the transition temperature of the bulk system. The region in between the  $3D$  to  $0D$  crossover uncovers the contributions from the surface and the edges of the cylindrical boxes. Our finite size scaling analysis of the specific heat and London penetration depth of high quality  $\text{YBa}_2\text{Cu}_3\text{O}_{7-\delta}$  and  $\text{Bi}_2\text{Sr}_2\text{CaCu}_2\text{O}_{8+\delta}$  single crystals uncover essentially the same crossover phenomena, including evidence for surface and edge contributions. This implies that the bulk samples break into nearly homogeneous superconducting grains of rather unique extent and with that granular superconductivity.

To appear in the proceedings of Symmetry and Heterogeneity in High Temperature Superconductors, Erice-Sicily:  
4-10 October 2003

Since the discovery of superconductivity in cuprates by Bednorz and Müller [1] a tremendous amount of work has been devoted to their characterization. The issues of inhomogeneities, granularity, and their characterization are essential for several reasons, including: (I) If inhomogeneity is an intrinsic property, a re-interpretation of experiments, measuring an average of the electronic properties, is unavoidable. (II) Inhomogeneity may point to a microscopic phase separation, i.e. superconducting grains, embedded in a non-superconducting matrix. (III) There is neutron spectroscopic evidence for nanoscale cluster formation and percolative superconductivity in various cuprates [2,3]. (IV) Nanoscale spatial variations in the electronic characteristics have been observed on the surface of  $\text{Bi}_2\text{Sr}_2\text{CaCu}_2\text{O}_{8+\delta}$  with scanning tunnelling microscopy (STM) [4–7]. They reveal a spatial segregation of the electronic structure into 3nm diameter superconducting domains in an electronically distinct background. (V) Remarkably, in the experimentally accessible temperature regime, the critical properties of the superconductor to normal state transition are found to fall into the 3D-XY universality class, except from a rounding of the transition [9,8,10–25]. This, however, is the result expected according to the Harris criterion [26], which states that short-range correlated and uncorrelated disorder is irrelevant at the unperturbed critical point, provided that the specific heat exponent  $\alpha$  is negative. Since in the 3D-XY universality class  $\alpha$  is negative [27], the rounding of the transition appears then to uncover a finite size effect [28,29]. Indeed, consistency of the rounded transition in the specific heat and penetration depths with a finite size effect has been established in a variety of cuprate superconductors. The finite size scaling analysis revealed that homogeneity is restricted to grains with nanoscale extension [22,30–34]. (VI) On the other hand, single crystals of cuprate superconductors conduct in the normal state along any direction. Accordingly, bulk superconductivity requires the grains to percolate. (VII) If this finite size scenario holds true, the finite size behavior of the superconductor to normal state transition should resemble features of the superfluid transition of confined  $^4\text{He}$ , which falls into the 3D-XY universality class, as well [35–38]. In particular, the finite size effect should also provide information on the geometry of the grains, e.g. their surface, edges, corners, etc. (VIII) Noting that in  $\text{Y}_{1-x}\text{Pr}_x\text{Cu}_3\text{O}_{7-\delta}$  [30] and  $\text{YBa}_2\text{Cu}_4\text{O}_8$  [34] the transition temperature increases with reduced extent of the grains along the  $c$ -axis, the geometry turns out to be a relevant feature. Indeed, if the grain is in contact with a superconducting layer with a higher " $T_c$ ", superconductivity is predicted to be enhanced and  $T_c$  increases with reduced radius of curvature of the grains [39].

In this paper we review and refine the evidence for finite size behavior in the specific heat and penetration depth data of cuprate superconductors. Since  $^4\text{He}$  confined to uniform small dimensions has been the subject of fundamental research for over three decades, we sketch next the finite size scaling analysis of the specific heat of  $^4\text{He}$  confined to cylindrical boxes whose diameter and height are  $1\mu\text{m}$  [38]. This provides information on a system where confinement is made by design and modifies its critical behavior, while other effects such as disorder are not present. Close to the bulk transition temperature  $T_c$  the singular part of the specific heat adopts the form

$$c_b(t) = c_{bs}(t) + B^\pm, \quad c_{bs}(t) = \frac{A^\pm}{\alpha} |t|^{-\alpha}. \quad (1)$$

$t = 1 - T/T_c$  is the reduced temperature,  $A^\pm$  the critical amplitude and  $\alpha$  the critical exponent of the specific heat, while  $B^\pm$  arises from the background, and  $\pm = \text{sgn}(t)$ .

Since superconductors in the experimentally accessible critical regime and  $^4\text{He}$  fall into the 3D-XY universality class, with known critical exponents and critical amplitude combinations, we take these properties for granted [27]. They include the exponents

$$\alpha = 2 - 3\nu = -0.013, \quad \nu = 0.671, \quad (2)$$

and the critical amplitude combinations

$$A^\pm V_c^\pm = (R^\pm)^3, \quad V_c^\pm = (\xi_0^\pm)^3, \quad (3)$$

where

$$\frac{A^+}{A^-} = 1.07, \quad R^- = 0.815, \quad R^+ = 0.361. \quad (4)$$

$\xi_0^\pm$  is the critical amplitude of the correlation length, diverging in the bulk system as  $\xi^\pm = \xi_0^\pm |t|^{-\nu}$ , and  $V_c^\pm = (\xi_0^\pm)^3$  is the correlation volume.

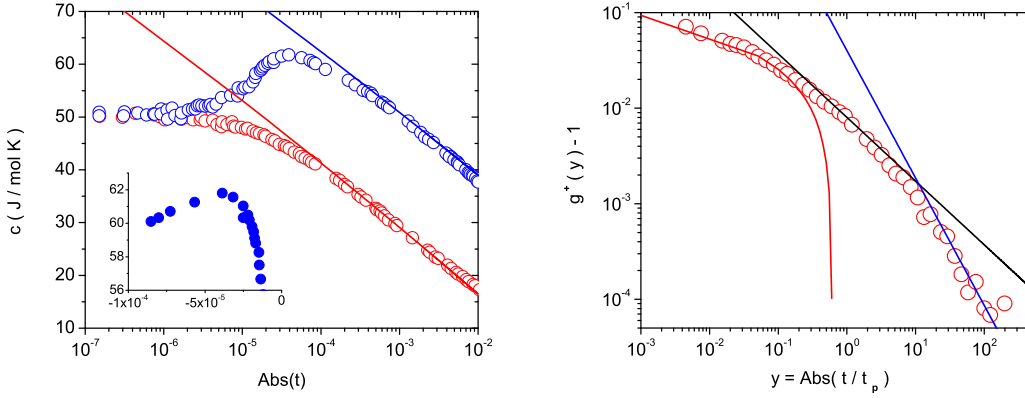


FIG. 1. (a) Specific heat  $c$  of  $^4\text{He}$  confined to  $1\mu\text{m}^3$  cylindrical boxes versus  $|t|$  compared to the bulk data. The lines represent the bulk data and the open symbols are the confined system. Taken from Kimball *et al.* [38]. The insertion shows  $c$  versus  $t$  around  $t_p \approx -3.9 \cdot 10^{-5}$ . (b) Corresponding finite size scaling function  $g^+(y) - 1$  versus  $y = |t/t_p|$ . The red curve indicates the limiting behavior  $g^+(|y| \rightarrow 0) = g_0^+ |y|^{-|\alpha|}$  in terms of  $g^+ = 0.993 |y|^{-0.014}$ . The black line,  $g^+(y) - 1 = 0.008 |y|^{-2/3}$  uncovers the surface and the blue one,  $g^+(y) - 1 = 0.04 |y|^{-4/3}$  the edge contributions.

Fig.1a shows the specific heat of  $^4\text{He}$  confined to  $1\mu\text{m}^3$  cylindrical boxes and contrasts it to the unconfined system, the solid lines [38]. The lower branch corresponds to  $T > T_c$  and the upper to  $T < T_c$ . Notice at large values of  $|t|$ , the data match the bulk data. As one moves closer to the bulk transition, the confined systems specific heat begins to systematically deviate from the bulk data. This is predicted by finite-size scaling theory [29,28]. As the system feels its finite size when the correlation length  $\xi$  becomes of the order of the smallest confining length, the specific heat adopts the scaling form, asserting that

$$\frac{c_b(t) - c(t, L)}{|c_{bs}(t)|} = g^\pm(y) - 1, \quad y = t/|t_p|, \quad |t_p| = (\xi_0^-/L)^{1/\nu}. \quad (5)$$

$g^\pm(y)$  is the finite size scaling function which satisfies:  $g^-(-1) = 1$  at  $T = T_p$ , where  $\xi^-(t_p) = \xi_0^- |t_p|^{-\nu} = L$ , so that  $y = y_p = -1$ , while  $g^\pm(y \rightarrow 0) = g_0^\pm |y|^{-|\alpha|}$  holds for  $\alpha < 0$  and  $g^\pm(|y| \rightarrow \infty) = 1$ .  $L$  is the smallest spatial length of the confined system.  $g^+(y)$ , derived from the data of Kimball *et al.* [38], is displayed in Fig.1b. The red curve indicates the 0D limiting behavior  $g^+(|y| \rightarrow 0) = g_0^+ |y|^{-|\alpha|}$ . In between these limits, where the correlation length is smaller than  $L$ , so that  $|t| \gtrsim |t_p|$ , the free energy density (and other thermodynamic quantities) can be expanded in  $D = 3$  as [29]

$$f(t, L) - f_b(t) = \frac{1}{L} f_s(t) + \frac{1}{L^2} f_e(t) + \frac{1}{L^3} f_c(t). \quad (6)$$

The contributions  $f_s$ ,  $f_e$  and  $f_c$  can be attributed to the surfaces, edges and corners of the confinement. It is expected that each one of these terms contribute in a limited region of the scaling variable. Since  $f_s$  and  $f_e$  scale as  $\xi^{-2}$  and  $\xi^{-1}$ , their contribution to the specific heat  $c \propto -\partial^2 f / \partial t^2$  scales as  $|t|^{-\alpha-\nu}$  and  $|t|^{-\alpha-2\nu}$ , respectively. Hence the surface term should behave as  $|t/t_p|^{-\nu}$  and the edge term as  $|t/t_p|^{-2\nu}$  in the scaling form, Eq. (5). A glance to Fig.1b shows that as one proceeds to smaller values of the scaling variable  $y = |t/t_p|$  there is clear evidence for crossovers from the edges,  $\propto |t/t_p|^{-4/3}$ , to the surface,  $\propto |t/t_p|^{-2/3}$ , contribution and finally to the asymptotic behavior,  $g^+ (|y| \rightarrow 0) = g_0^+ |y|^{-|\alpha|}$ . Thus, the finite size scaling function does not uncover the crossover from 3D to 0D behavior only, but allows to identify surface and edge contributions, as well.

We have seen that  $^4\text{He}$  confined to  $1\mu\text{m}^3$  cylindrical boxes crosses over from a 3D to a 0D behavior near the bulk transition. This has a marked effect on the specific heat as seen by the pronounced rounding of the peak and its shift to a temperature lower than the transition of the bulk system. Furthermore, the region in between the 3D to 0D crossover uncovers the contributions from the surface and the edges of the cylindrical boxes. Since disorder is not present, the modifications of the critical behavior are entirely due to the confinement. Analogous behavior in cuprate superconductors would imply that the bulk breaks into homogeneous superconducting grains with rather unique extent, embedded in a nonsuperconducting matrix.

In Fig.2 we show the specific heat data of Charalambous *et al.* [40] of a high quality  $\text{YBa}_2\text{Cu}_3\text{O}_{7-\delta}$  single crystal in terms of the specific heat coefficient  $c/T$  versus  $|t|$ . Comparing Figs.1a and 2 we observe: (i) in  $\text{YBa}_2\text{Cu}_3\text{O}_{7-\delta}$  the rounding of the transition sets in at much higher reduced temperatures; (ii) otherwise the rounding is remarkably analogous to that of  $^4\text{He}$  confined to  $1\mu\text{m}^3$  cylindrical boxes. Noting that in  $^4\text{He}$  and optimally doped  $\text{YBa}_2\text{Cu}_3\text{O}_{7-\delta}$  the critical amplitude  $\xi_0^-$  are comparable, the relation  $|t_p| = (\xi_0^-/L)^{1/\nu}$  (Eq.2) indicates that the difference in the onset of the rounding is due to a limiting length scale, considerably smaller than the  $1\mu\text{m}$  in  $^4\text{He}$ .

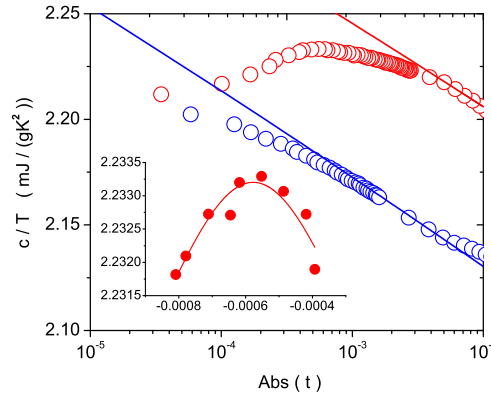


FIG. 2. Specific heat coefficient  $c/T$  of the high quality  $\text{YBa}_2\text{Cu}_3\text{O}_{7-\delta}$  single crystal (sample UBC2) versus  $|t|$  taken from Charalambous *et al.* [40]. The solid lines represent the expected behavior of a fictitious homogeneous bulk sample according to Eq.(1). The insertion shows  $c/T$  versus  $t$  around  $t_p \approx -5.8 \cdot 10^{-4}$ .

To substantiate and refine the consistency with a finite size effect further we displayed in Fig.3 the scaling functions  $g^-(y) - 1$  and  $g^+(y) - 1$ . As one proceeds to smaller values of the scaling variable  $y = |t/t_p|$  there is, in analogy to  $^4\text{He}$  confined to  $1\mu\text{m}^3$  cylindrical boxes (Fig.1b), clear evidence for crossovers from the edge,  $\propto |t/t_p|^{-4/3}$ , to the surface,  $\propto |t/t_p|^{-2/3}$ , contributions and finally to the 0D behavior,  $g^+ (|y| \rightarrow 0) = g_0^+ |y|^{-|\alpha|}$ .

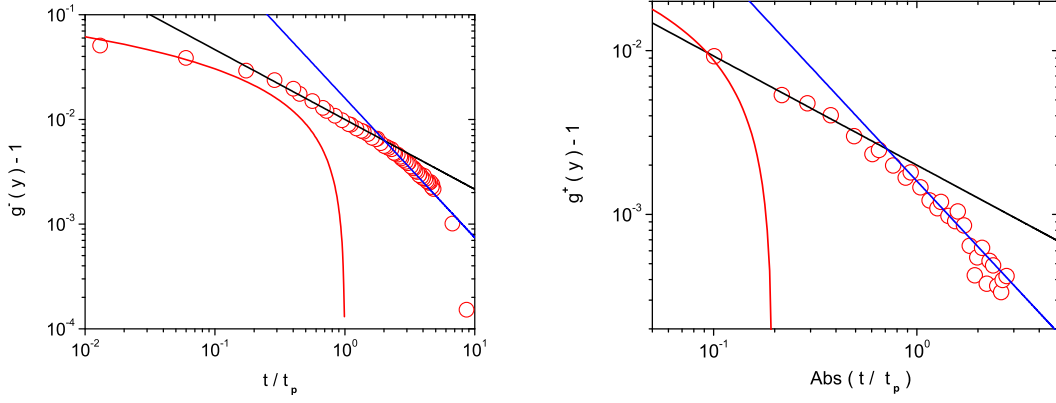


FIG. 3. (a)  $g^-(y) - 1$  versus  $y = t/t_p$  derived from the data shown in Fig.2. The red curve indicates the limiting behavior  $g^-(|y| \rightarrow 0) = g_0^- |y|^{-|\alpha|}$  in terms of  $g^+ = |y|^{-0.013}$ . The black line,  $g^-(y) - 1 = 0.01 |y|^{-2/3}$  uncovers the surface and the blue one,  $g^-(y) - 1 = 0.016 |y|^{-4/3}$  the edge contributions. (b)  $g^+(y) - 1$  versus  $y = |t/t_p|$  derived from the data shown in Fig.2. The red curve indicates the limiting 0D behavior,  $g^+(|y| \rightarrow 0) = |y|^{-0.013}$ . The black line,  $g^+(y) - 1 = 0.002 |y|^{-2/3}$  corresponds to the surface and the blue one,  $g^+(y) - 1 = 0.0016 |y|^{-4/3}$ , to the edge contributions.

When this finite size scenario holds true, the London penetration depth should not only exhibit a rounded transition, consistent with a finite size effect [30–34], but uncover the surface and edge contributions, as well. Considering again the 3D-XY critical point, extended to the anisotropic case, the penetration depths and transverse correlation lengths in directions  $i$  and  $j$  are universally related by [22,41]

$$\frac{1}{\lambda_i(T) \lambda_j(T)} = \frac{16\pi^3 k_B T}{\Phi_0^2 \sqrt{\xi_i^t(T) \xi_j^t(T)}}. \quad (7)$$

A limiting length scale  $L_i$  in direction  $i$  implies that  $\xi_i^t \xi_j^t$  does not diverge but is bounded by  $\xi_i^t \xi_j^t = (\xi_k^-)^2 \leq L_k^2$ , where  $i \neq j \neq k$ .  $\xi_i^t$  denotes the transverse and  $\xi_k^- = \sqrt{\xi_i^t \xi_j^t}$  the corresponding real space correlation length. The resulting finite size effect has been established in a variety of cuprates [30–34]. Here we refine these studies to identify surface and edge contributions. As first example we consider the high-quality  $\text{Bi}_2\text{Sr}_2\text{CaCu}_2\text{O}_{8+\delta}$  single crystal data of Jacobs *et al.* [42] shown in Fig.4. The solid curve indicates the leading critical behavior of the fictitious homogeneous system with  $T_c = 87.5\text{K}$ , while the rounded transition points to a finite size effect. A characteristic feature of a finite size effect in  $1/\lambda_{ab}^2(T)$  is the occurrence of an inflection point giving rise to an extremum in  $d(\lambda_{ab}^2(T=0)/\lambda_{ab}^2(T))/dT$  at  $T_p$ . Here Eq.(7) reduces to

$$\frac{1}{\lambda_{ab}^2(T_p)} \approx \frac{1}{\lambda_a(T_p) \lambda_b(T_p)} = \frac{16\pi^3 k_B T_p}{\Phi_0^2 L_c}. \quad (8)$$

The data shown in Fig.4 exhibits in  $d(\lambda_{ab}^2(T=0)/\lambda_{ab}^2(T))/dT$  at  $T_p \approx 87\text{K}$  an extremum and with that an inflection point in  $1/\lambda_{ab}^2(T)$ . With  $\lambda_{ab}(T=0) = 1800\text{\AA}$  as obtained from  $\mu\text{SR}$  measurements [43] and  $\lambda_{ab}^2(T=0)/\lambda_{ab}^2(T_p) = 0.066$  we find  $L_c \approx 68\text{\AA}$ .

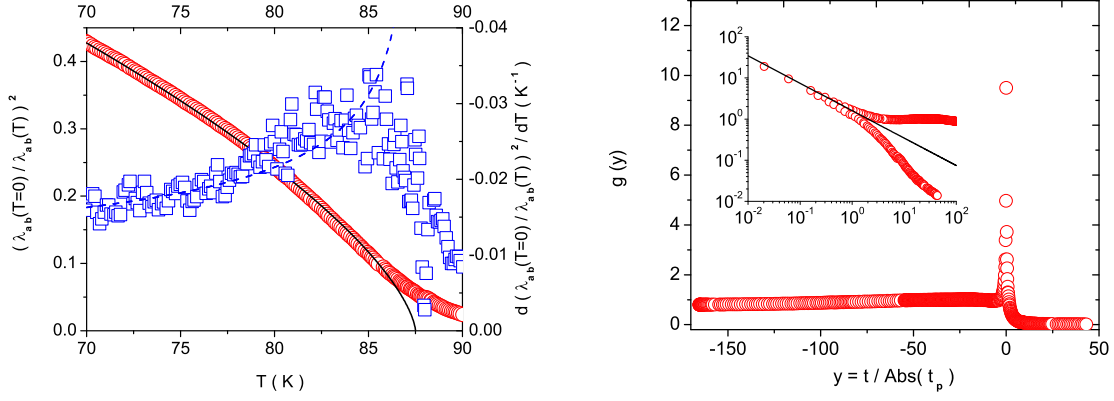


FIG. 4. (a) Microwave surface impedance data for  $\lambda_{ab}^2(T=0)/\lambda_{ab}^2(T)$  ( $\circ$ ) and  $d(\lambda_{ab}^2(T=0)/\lambda_{ab}^2(T))/dT$  ( $\square$ ) versus  $T$  of a high-quality  $\text{Bi}_2\text{Sr}_2\text{CaCu}_2\text{O}_{8+\delta}$  single crystal taken from Jacobs *et al.* [42]. The solid line is  $\lambda_{ab}^2(0)/\lambda_{ab}^2(T) = 1.2(1 - T/T_c)^{2/3}$  with  $T_c = 87.5\text{K}$  and the dashed line its derivative indicating the leading critical behavior of the fictitious homogeneous system. The rounded transition exhibits an inflection point at  $T_p \approx 87\text{K}$ , where  $d(\lambda_{ab}^2(0)/\lambda_{ab}^2(T))/dT$  is maximum. (b) Scaling function  $g(y) = (\lambda_{0ab}/\lambda_{ab}(T))^2 |t|^{-\nu}$  versus  $y = t/|t_p|$  for the data shown in Fig.4a. The solid line in the insertion is Eq.(10) with  $g_0 = 1.6$ . It indicates the flow to the 0D behavior.

To strengthen the evidence for a finite size effect we explore next the consistency of the data with the corresponding finite size scaling function. In the present case it is defined as

$$\left(\frac{\lambda_{0ab}}{\lambda_{ab}(T, L_c)}\right)^2 |t|^{-\nu} = g^\pm(y), \quad y = \text{sign}(t) \left|\frac{t}{t_p}\right|. \quad (9)$$

For  $t$  small and  $L_c \rightarrow \infty$ , so that  $\pm y \rightarrow \infty$  it should tend to  $g^-(y \rightarrow -\infty) = 1$  and  $g^+(y \rightarrow \infty) = 0$ , respectively, while for  $t = 0$  and  $L \neq 0$  it diverges as

$$g^\pm(y \rightarrow 0) = g_0^\pm |y|^{-\nu}. \quad (10)$$

In this 0D limit,  $(\lambda_{0ab}/\lambda_{ab}(T_c, L_c))^2 = g_0^- |t_p|^\nu = g_0^- \xi_{0c}^-/L_c$ . Moreover at  $t_p$ ,  $y = -1$  and  $d(\lambda_{0ab}/\lambda_{ab}(T, L))^2/dt = 0$ . The scaling function shown in Fig.4b, derived from the data shown in Fig.4a, is apparently fully consistent with the limiting behavior of the finite size scaling function and uncovers, in analogy  $^4\text{He}$ , confined to cylindrical boxes, a 3D to 0D crossover. On the other hand, in analogy to the specific heat, refined information may be attained in between these limits. Here the correlation length is smaller than  $L_c$ ,  $|t| \gtrsim |t_p|$ , and the contributions from the surface and edges should become observable. Since  $f_s$  and  $f_e$  scale as  $1/(L\xi^2)$  and  $1/(L^2\xi)$ , their contributions to  $1/\lambda^2 \propto f \xi^2$  scale as  $1/L$  and  $\xi/L$ , respectively. Hence the surface term should behave as  $|t/t_p|^{-\nu}$  and the edge term as  $|t/t_p|^{-2\nu}$  in the scaling form, Eq. (9). A glance to Fig.5 shows that as one proceeds to smaller values of the scaling variable  $y = |t/t_p|$  there is indeed evidence for crossovers from the edges,  $\propto |t/t_p|^{-4/3}$ , to the surface,  $\propto |t/t_p|^{-2/3}$ , contributions and finally to the 0D behavior,  $g^+ (|y| \rightarrow 0) = g_0^+ |y|^{-2/3}$ .

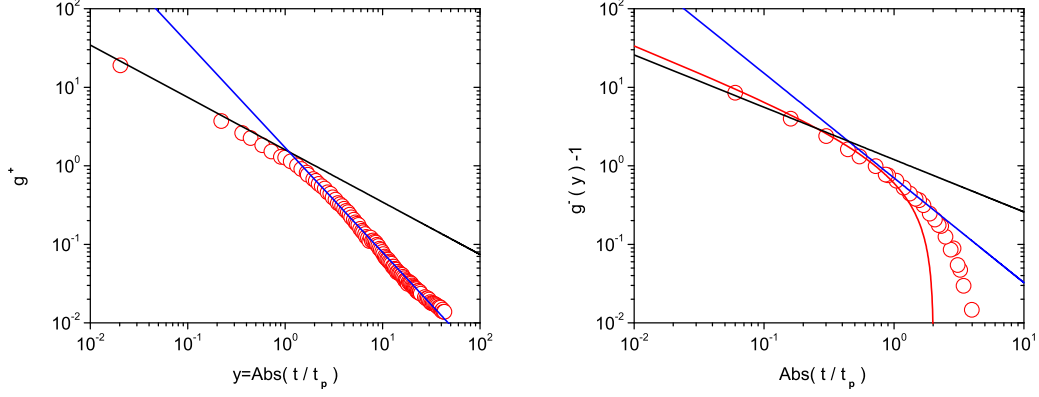


FIG. 5. (a) Scaling function  $g^+(y)$  versus  $y = |t/t_p|$  derived from the data shown in Fig.4. The blue line,  $g^+(y) = 1.7y^{-4/3}$  corresponds to the edge and the black one,  $g^+(y) = 1.6y^{-2/3}$ , to the surface contribution. (b)  $g^-(y) - 1$  versus  $y = |t/t_p|$  derived from the data shown in Fig.4. The blue line,  $g^-(y) - 1 = 0.7y^{-4/3}$ , indicates the edge, the black one,  $g^-(y) - 1 = 1.2y^{-2/3}$ , the surface contribution and the red curve indicates the flow to the 0D behavior,  $g^-(y) = 1.6y^{-2/3}$ .

As second example we treat the in-plane penetration depth data of Kamal *et al.* [14] for a high-quality  $\text{YBa}_2\text{Cu}_3\text{O}_{6.95}$  single crystal. In Fig.6a we displayed the data in terms of  $1/\lambda_{ab}^2(T)$  and  $d(1/\lambda_{ab}^2(T))/dT$  versus  $T$ . The red and blue curves indicate the leading critical behavior of the fictitious homogeneous system with  $T_c = 88.65\text{K}$ , while the rounded transition points to a finite size effect. The occurrence of an extremum in  $d(1/\lambda_{ab}^2(T))/dT$  at  $T_p \approx 88.52\text{K}$  is a characteristic feature of a finite size effect in  $1/\lambda_{ab}^2(T)$ , giving rise to an inflection point in  $1/\lambda_{ab}^2(T)$  at  $T_p$ . Using  $1/\lambda_{ab}^2(T_p) = 0.918 (\mu\text{m})^{-2}$ , we deduce with the aid of Eq.(8) for the limiting length scale along the c-axis the estimate  $L_c = 154\text{\AA}$ . The associated scaling function  $g(y)$ , defined in Eq.(9), is shown in Fig.6b. As one proceeds to smaller values of the scaling variable  $y$  there is in the lower branch ( $T > T_c$ ) clear evidence for a crossover from the edge,  $\propto |t/t_p|^{-4/3}$ , to the surface,  $\propto |t/t_p|^{-2/3}$ , contributions.

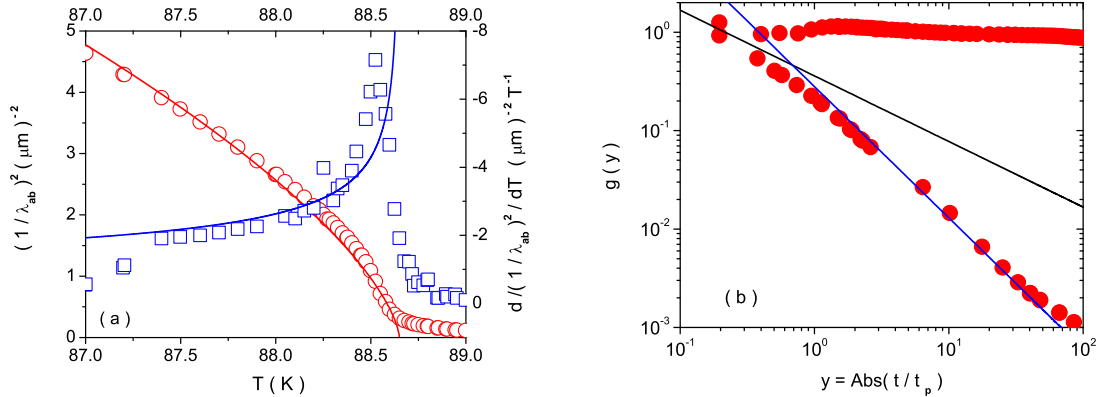


FIG. 6. (a) In-plane penetration depth data for  $1/\lambda_{ab}^2(T)$  ( $\circ$ ) and  $d(1/\lambda_{ab}^2(T))/dT$  ( $\square$ ) versus  $T$  of a high-quality  $\text{YBa}_2\text{Cu}_3\text{O}_{6.95}$  single crystal taken from Kamal *et al.* [14]. The solid line is  $1/\lambda_{ab}^2(T) = 68(1 - T/T_c)^{2/3}$  with  $T_c = 88.65\text{K}$  and the dashed line its derivative indicating the leading critical behavior of the fictitious homogeneous bulk system. The rounded transition exhibits an inflection point at  $T_p \approx 88.52\text{K}$ , where  $d(1/\lambda_{ab}^2(T))/dT$  is maximum. (b) Scaling function  $g(y) = (\lambda_{0ab}/\lambda_{ab}(T))^2 |t|^{-\nu}$  versus  $y = t/|t_p|$  for the data shown in Fig.4a. The black line,  $g^+(y) = 0.36y^{-2/3}$ , indicates the surface and the blue one,  $g^+(y) = 0.28y^{-4/3}$ , the edge contributions above  $T_c$ .

We reviewed and refined the finite size scaling analysis of specific heat and London penetration depths data of cuprate superconductors and compared them to the analysis of specific heat measurements near the superfluid transition of  $^4\text{He}$  confined to  $1\mu\text{m}^3$  cylindrical boxes. The  $^4\text{He}$  system provides information on a system where confinement is made deliberately. It modifies its critical behavior while other effects such as disorder are not present. We have seen that this system crosses from 3D to 0D behavior near the transition. As a result of this crossover, the specific heat peak

exhibits a pronounced rounding and the maximum shifts to a temperature lower than the transition temperature of the bulk system. The region in between the 3D to 0D crossover uncovered contributions from the surface and the edges of the cylindrical boxes. The analysis of the specific heat and London penetration depth of high quality  $\text{YBa}_2\text{Cu}_3\text{O}_{7-\delta}$  and  $\text{Bi}_2\text{Sr}_2\text{CaCu}_2\text{O}_{8+\delta}$  single crystals uncovered essentially the same crossover phenomena, including evidence for surface and edge contributions. No new critical behavior emerges, but 3D-XY scaling is achieved with the variable  $\xi/L$ , where  $L$  is the smallest confining dimension. This implies that the bulk samples break into nearly homogeneous superconducting grains of rather unique extent and with that granular superconductivity.

## ACKNOWLEDGMENTS

The author is grateful to D. Di Castro, R. Khasanov, H. Keller, K.A. Müller and J. Roos for very useful comments and suggestions on the subject matter.

- 
- [1] G. Bednorz and K. A. Müller, Z. Phys. B **64**, 189 (1986).
  - [2] J. Mesot, P. Allensbach, U. Staub and A. Furrer, Phys. Rev. Lett. **70**, 865 (1993).
  - [3] A. Furrer *et al.*, Physica C **235-240**, 261 (1994).
  - [4] J. Liu, J. Wan, A. Goldman, Y. Chang and P. Jiang, Phys. Rev.Lett. **67**, 2195 (1991).
  - [5] A. Chang, Z. Rong, Y. Ivanchenko, F. Lu and E. Wolf, Phys. Rev. B **46**, 5692 (1992).
  - [6] T. Cren, D. Roditchev, W. Sacks, J. Klein, J.-B. Moussy, C. Deville-Cavellin, and M. Laguës, Phys. Rev. Lett. **84**, 147 (2000).
  - [7] K. M. Lang, V. Madhavan, J. E. Hoffman, E. W. Hudson, H. Eisaki, S. Uchida and J. C. Davis, Nature **415**, 413 (2002).
  - [8] D.S. Fisher, M.P.A. Fisher, and D.A. Huse, Phys. Rev. B **43**, 130 (1991).
  - [9] T. Schneider and D. Ariosa, Z. Phys. B **89**, 267 (1992).
  - [10] T. Schneider and H. Keller, Int. J. Mod. Phys. B **8**, 487 (1993).
  - [11] N. Overend, M.A. Howson, and I.D. Lawrie, Phys. Rev. Lett. **72**, 3238 (1994).
  - [12] M. A. Hubbard, M. B. Salamon, and B. W. Veal, Physica C **259**, 309 (1996).
  - [13] Y. Jaccard, T. Schneider, J.-P. Looquet, E. J. Williams, P. Martinoli and O. Fischer., Europhys. Lett., **34**, 281 (1996).
  - [14] S. Kamal, D. A. Bonn, N. Goldenfeld, P. J. Hirschfeld, R. Liang and W. N. Hardy., Phys. Rev. Lett. **73**, 1845 (1994).
  - [15] S. Kamal, R. Liang, A. Hosseini, D. A. Bonn, and W. N. Hardy, Phys. Rev. B **58**, 8933 (1998).
  - [16] V. Pasler, P. Schweiss, Ch. Meingast, B. Obst, H. Wühl, A. I. Rykov, and S. Tajima, Phys. Rev. Lett. **81**, 1094 (1998).
  - [17] T. Schneider, J. Hofer, M. Willemin, J.M. Singer, and H. Keller, Eur. Phys. J. B **3**, 413 (1998).
  - [18] T. Schneider and J. M. Singer, Physica C **313**, 188 (1999).
  - [19] J. Hofer, T. Schneider, J. M. Singer, M. Willemin, H. Keller, Ch. Rossel, and J. Karpinski, Phys. Rev. B **60**, 1332 (1999).
  - [20] J. Hofer, T. Schneider, J. M. Singer, M. Willemin, H. Keller, T. Sasagawa, K. Kishio, K. Conder and J. Karpinski, Phys. Rev. B **62**, 631 (2000).
  - [21] T. Schneider and J. S. Singer, Physica C **341-348**, 87 (2000).
  - [22] T. Schneider and J. M. Singer, *Phase Transition Approach To High Temperature Superconductivity*, Imperial College Press, London, 2000.
  - [23] Ch. Meingast, V. Pasler, P. Nagel, A. Rykov, S. Tajima, and P. Olsson, Phys. Rev. Lett. **86**, 1606 (2001).
  - [24] T. Schneider, Physica B **326**, 289 (2003).
  - [25] K. D. Osborn, D. J. Van Harlingen, Vivek Aji, N. Goldenfeld, S. Oh, and J. N. Eckstein, Phys. Rev. B **68**, 144516 (2003).
  - [26] A. B. Harris, J. Phys. C **7**, 1671 (1974).
  - [27] A. Peliasetto and E. Vicari, Physics Reports **368**, 549 (2002).
  - [28] J. L. Cardy ed., *Finite-Size Scaling*, North Holland, Amsterdam 1988.
  - [29] V. Privman, *Finite Size Scaling and Numerical Simulations of Statistical Systems*, World Scientific, NJ, 1990.
  - [30] T. Schneider, R. Khasanov, K. Conder, and H. Keller, J. Phys. Condens. Matter **15**, L763 (2003).
  - [31] T. Schneider, cond-mat/0308595.
  - [32] T. Schneider and D. Di Castro, Phys. Rev. B **69**, 024502 (2004).
  - [33] T. Schneider, Journal of Superconductivity, **17**, 41 (2004).
  - [34] R. Khasanov, T. Schneider, and H. Keller, cond-mat/
  - [35] M. Coleman and J. A. Lipa, Phys. Rev. Lett. **74**, 286 (1995).
  - [36] A. M. Kahn and G. Ahlers, Phys. Rev. Lett. **74**, 944 (1995).

- [37] D. Murphy, E. Genio, G. Ahlers, F. Liu, and Y. Liu, Phys. Rev. Lett. **90**, 025301 (2003).
- [38] M. O. Kimball, M. Diaz-Avila, and F. M. Gasparini, Physica B **329-333**, 286 (2003).
- [39] E. Montevocchi and J.O. Indekeu, Phys. Rev. B **62**, 14359 (2000).
- [40] M. Charalambous, O. Riou, P. Gandit, B. Billon, P. Lejay, J. Chaussy, W. N. Hardy, D. A. Bonn, and R. Liang, Phys. Rev. Lett. **83**, 2042 (1999).
- [41] P. C. Hohenberg, A. Aharony, B. I. Halperin and E. P. Siggia, Phys. Rev. B **13**, 2986 (1976).
- [42] T. Jacobs, S. Sridhar, Q. Li, G. D. Gu, N. Koshizuka, Phys. Rev. Lett. **75**, 4516 (1995).
- [43] Shih-Fu Lee, D. C. Morgan, R. J. Ormeno, D. M. Broun, R. A. Doyle, J. R. Waldram, and K. Kadowaki, Phys. Rev. Lett. **71**, 3862 (1993).